sustainability

MDPI

Article

Heat Transfer Studies on Solar Parabolic trough Collector Using Corrugated Tube Receiver with Conical Strip Inserts

Ramalingam Venkatesaperumal [1,*], Kutbudeen Syed Jafar [1], Perumal Venkatesan Elumalai [2], Mohamed Abbas [3,4], Erdem Cuce [5,6,*], Saboor Shaik [7] and Chanduveetil Ahamed Saleel [8]

1 Department of Mechanical Engineering, FEAT Annamalai University, Annamalainagar 608002, India
2 Department of Mechanical Engineering, Aditya Engineering College, Surampalem 533437, India
3 Electrical Engineering Department, College of Engineering, King Khalid University, Abha 61421, Saudi Arabia
4 Electronics and Communications Department, College of Engineering, Delta University for Science and Technology, Gamasa 35712, Egypt
5 Low/Zero Carbon Energy Technologies Laboratory, Faculty of Engineering and Architecture, ZihniDerin Campus, Recep Tayyip Erdogan University, Rize 53100, Turkey
6 Department of Mechanical Engineering, Faculty of Engineering and Architecture, ZihniDerin Campus, Recep Tayyip Erdogan University, Rize 53100, Turkey
7 School of Mechanical Engineering, Vellore Institute of Technology, Vellore 632014, India
8 Department of Mechanical Engineering, College of Engineering, King Khalid University, P.O. Box 394, Abha 61421, Saudi Arabia
* Correspondence: rvplme1977@gmail.com (R.V.); erdem.cuce@erdogan.edu.tr (E.C.); Tel.: +90-464-2237518-1203 (E.C.); Fax: +90-464-2237514 (E.C.)

Abstract: The heat transfer characteristics of the working fluid passing through the absorber of a solar parabolic trough collector (SPTC) can be enhanced by the creation of a turbulence effect. Therefore, a novel idea was implemented by introducing a corrugated tube (CT) absorber instead of a plain tube absorber in a solar parabolic trough collector. The heat transfer enhancement was improved further through the use of conical strip inserts inside the corrugated tube absorber of the SPTC. A corrugated tube (CT) receiver with a pitch of 8 mm and corrugation height of 2 mm was used with three different pitches of conical strip inserts (pitch pi = 20 mm, 30 mm and 50 mm) for the analysis of the thermal performance of the SPTC. Initially, experiments were conducted in a plain tube and corrugated tube receiver at different mass flow rates. The convective heat transfer rate was increased for all the configurations of the conical strip inserts. The SPTC performance was good for the combination of the corrugated tube (pc = 8 mm and hc = 2 mm) and the conical strip insert I3 (pi = 20 mm). The experimental results showed that the maximum achieved Nu value, friction factor, instantaneous efficiency and thermal efficiency of the CT-I3 were 177%, 38%, 26.92% and 9% compared to the plain tube under the same working conditions.

Keywords: solar parabolic trough collector; plain tube receiver; corrugated tube receiver; transient flow; conical strip inserts

Citation: Venkatesaperumal, R.; Syed Jafar, K.; Elumalai, P.V.; Abbas, M.; Cuce, E.; Shaik, S.; Saleel, C.A. Heat Transfer Studies on Solar Parabolic trough Collector Using Corrugated Tube Receiver with Conical Strip Inserts. *Sustainability* **2023**, *15*, 378. https://doi.org/10.3390/su15010378

Academic Editor: Kian Jon Chua

Received: 25 October 2022
Revised: 6 December 2022
Accepted: 17 December 2022
Published: 26 December 2022

1. Introduction

Non-conventional sources of energy are broadly used in a variety of sectors such as domestic and commercial buildings for space heating and hot water generation [1,2]. Uncovered solar collectors are mainly used to heat swimming pools in summer [3–5]. Katsaprakkis et al. [6] used solar-combi systems to meet the thermal energy needs for hot water production and swimming pool heating. Katsaprakkis et al. [7] investigated the hybrid power plants used for thermal energy production for indoor space heating load coverage. The proposed solar-combi system was able to provide 100% of the annual heating load coverage of the examined building, with an annual contribution from the solar collectors higher than 45%. Arnaoutakis et al. [8] reviewed the technological advances in concentrating solar power systems. A comprehensive, systematic approach was applied

regarding the highly specialized developments which have taken place in all aspects of the technology. Advances in geometric optics for the enhancement of solar concentration and temperature were reviewed, along with receiver configurations for efficient heat transfer. In this way, the article focused on the need for technical and efficient solar energy use to achieve a green energy revolution. Numerous investigational works have been carried out on the augmentation of the thermal performance of solar parabolic trough collectors (SPTC) using different techniques. Atwarirawani et al. [9] analyzed a PTC with twisted inserts of plain, square cut, oblique delta-winglet and serrated forms. The observations showed that the serrated twisted tape produced the best results among the studied models. George et al. [10] conducted experiments on two PTCs, one with a black color coated aluminum receiver and the other without coating. The result showed that the coated receiver increased the thermal performance by 10%. Evangelosbellos et al. [11] analyzed the effect of the central cylindrical insert in a SPTC and concluded that the use of a higher diameter increased the pumping work and thermal efficiency. Ketantiwan et al. [12] investigated the different pitch values of inserts of the wire coil and achieved an increased turbulence effect inside the tube. The Reynolds number and Nu number were also increased. The value of the Nu number was increased by 330% with the increased value of the convective heat transfer coefficient. Çaglar et al. [13] investigated a PTC with two different reflective surfaces (chrome plated and an Al composite panel) and concluded that the composite aluminum reflector achieved better performance due to its higher reflectivity. The absorber tube with and without a glass cover was also studied. The absorber tube with a glass cover showed minimum thermal losses. Kalidasan et al. [14] analyzed a PTC using hinged blades in the absorber tube and found highly efficient performance compared to that of a conventional tube; the average instantaneous thermal efficiency was 69.33%. Yousif et al. [15] investigated a PTC receiver using twisted tape inserts and observed a high friction factor. A passive technique produced the turbulent flow inside the absorber tube. Abad et al. [16] enhanced the PTC performance using copper foam in the receiver. The pressure drop and Nu number were shown to increase during experimentation. A performance enhancement was also observed with a higher Re number. Younas et al. [17] enhanced the collector efficiency using incident solar radiation with the help of an automatic tracking system. Aravind et al. [18] conducted experimental work on a PTC using a cavity absorber. A performance enhancement was achieved with a glass cover. Aldulaimi et al. [19] conducted experiments, changing the diameter of single, dual and triple twisted tubes. The maximum heat transfer was achieved using TTT. Norouzi et al. [20] increased the solar energy absorption by rotating the absorber tube. Al_2O_3-therminol oil was used as a heat-carrying fluid. The Al absorber efficiency was 25% greater than that obtained using a steel tube, and 15% thermal efficiency was achieved by the selection of the optimal rotational speed. Anbu et al. [21] conducted experiments on a heat exchanger using spiraled rod inserts in the corrugated tubes. It was found that the Nu number and friction factor value increased by 75.66% and 79.81%, respectively, when using the maximum corrugation and minimum pitch (hc = 1 mm, Pc = 8 mm) compared to a conventional tube with DI water. Mohammed Almeshaal et al. [22] conducted experimental work on a thermosyphon solar water heating system with fully twisted tape (Y = 3), twisted up to a length of 1 m with spaces at the leading edge of 150 mm, 300 mm, 450 mm in length. The heat transfer rate reduction for the L-R screw with a rod for a spacer length of 300 mm and 450 mm was 24% and 33%, respectively. The friction factor decreased by 53% and 56%, respectively. Yilmaz et al. [23] conducted experiments using a wire coil insert with therminol oil as the working fluid. The Nu number was increased by 183%, the thermal efficiency was increased by 1% and the average friction factor was increased by 14.41 times compared to the plain tube with water. Kumar et al. [24] analyzed the effect on the PTC performance of using a metal foam insert to change the mass flow rate; those authors reported that with their approach, the Nu number was increased 10 fold, the energy efficiency increased by 3.71% and thermal efficiency was increased 5 fold when compared to the conventional type. Wong et al. [25] investigated a corrugated tube receiver with a twisted tape insert in a PTC. CuO/water nanofluids were used as a HTF. The authors

noticed that the heat transfer rate increased by increasing the nanofluid concentration and decreasing the twist ratio. Several researchers have concentrated on various geometrical configurations of inserts and nanofluids to enhance the collector performance in SPTC. To date, no study has reported the effect of the use of a combination of a corrugated tube and conical strip inserts on various mass flow rates. Therefore, the present study analyzes the effect of combining a corrugated tube receiver (pc = 8 mm and hc = 2 mm) with conical strip inserts (pitch pi = 20 mm, 30 mm and 50 mm) under turbulent flow in a SPTC. Figure 1 shows the flow of the heat transfer fluid from the hot water storage tank (HWST) to the plain tube absorber of the SPTC through the pump and flow meter.

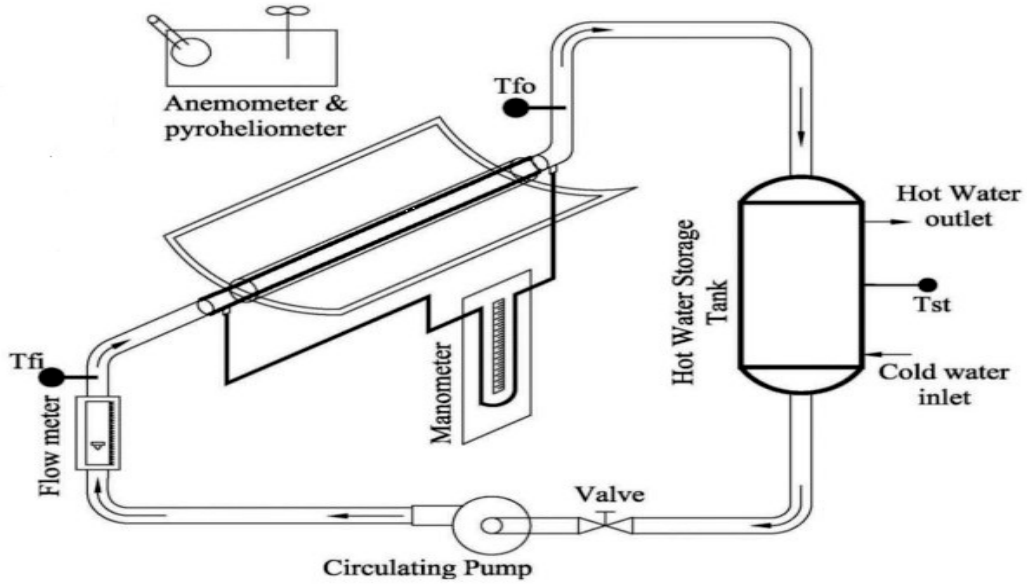

Figure 1. Schematic diagram of the solar PTC (plain tube).

2. Experimental Setup

The SPTC was prepared according to the specifications listed in Table 1 and shown in Figure 2. Experiments were carried out in Dharmapuri (12.1211° N, 78.1582° E), TN, India. The SPTC experimental setup used a corrugated tube absorber with a conical strip insert for the analysis of the friction factor, heat transfer and overall performance at different mass flow rates. The system consisted of a stainless-steel parabolic collector which focused solar radiation on a focal line through the reflective mechanism, a sun tracking system to focus the incident solar radiation, a hot water storage tank, a circulating pump, a flow measuring device and supporting and controlling devices. The conical strip insert was fitted with a corrugated tube and positioned at a 90° angle relative to the rim. It was enclosed using a glass cover to maximize the performance of the receiver. It received the focused solar radiation and transferred it to the working fluid. The pump circulated the water through the receiver in the circuit. The storage tank and pipeline were well insulated with glass wool. The SPTC was placed in the north–south direction to optimize its performance, i.e., to receive as much solar energy as possible [26,27]. The storage tank was filled to 70% capacity. Initially, the experiments were carried out using a plain tube copper receiver. Then, the experiments were continued with a corrugated tube as shown in Figure 3, and its specifications are listed in Table 2. Three different pitches of conical strip inserts were used with both the plain tube and corrugated tube are shown in Figure 4, and their specifications are listed in Table 3 (p_c = 8mm and h_c = 2mm). The results were tabulated and compared.

Table 1. SPTC Specifications.

Length of the collector (L)	2 m
Width of the Collector (w)	1 m
Focal distance (f)	0.25 m
Receiver inner diameter	18 mm
Receiver outer diameter	20 mm
Envelope cover inner diameter	22 mm
Envelope cover outer diameter	26 mm
Concentration ratio (C)	25.46
Absorptance of the receiver (α)	0.97
Emissivity of the receiver ($å_a$)	0.25
Envelope tube emissivity ($å_e$)	0.94
Tracking mechanism	Electronic type

Figure 2. Experimental setup of the solar PTC.

Figure 3. Photographic view of the corrugated tube.

Table 2. Geometrical specifications of the corrugated tube.

No.	Inner Diameter/Outer Diameter (mm)	Pitch p_c (mm)	Height h_c (mm)
CT	14/20	8	2

Two RTD PT 100 sensors were connected to the digital indicator (with 0.1°C accuracy), which measured the water temperature at the entry and exit of the receiver. A rotameter with an accuracy of ±1% measured the flow rate. An Eppley Pyrheliometer measured the intensity of solar radiation. A U-tube manometer measured the pressure of water at the entry and exit of the receiver. The reflectance of the stainless-steel material was enhanced to 0.974 by attaching solarflex foil on it. The black paint coated corrugated copper tube had an absorptance of 0.97, as tested using a double beam UV-VIS-NIR spectrophotometer at CECRI, Karaikudi, Tamil Nadu, India.

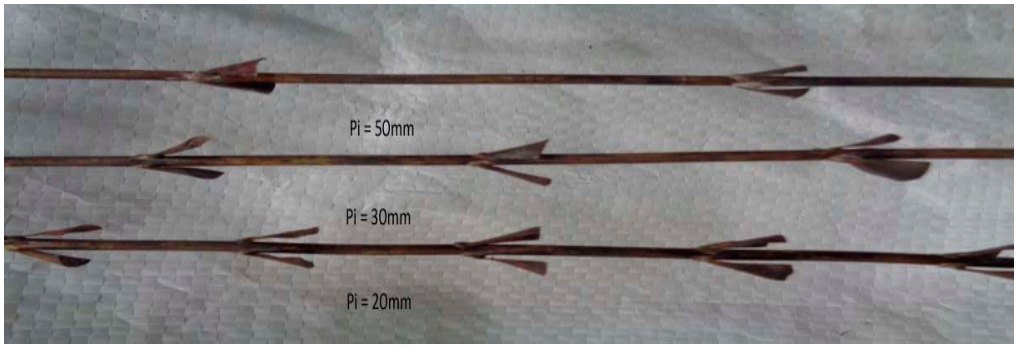

Figure 4. Photographic view of the conical strip inserts.

Table 3. Geometrical specifications of conical strip inserts.

No.	Diameter of Test Section (mm)	Pitch (mm)	The Angle of Inclination of the Strip
I_1	10	50	20°
I_2	10	30	20°
I_3	10	20	20°

3. Uncertainty Analysis

Uncertainty in the measured parameters affected the values of Re, Nu and f. Uncertainties in the measurements were estimated based on the procedure given by Holman [28]. In this study, the diameter of the tube (D), length of the tube (L), manometer readings (Δp), flow meter readings (ṁ) and thermometer readings (T1, T2) were noted. To determine the uncertainties in the experimental data, possible errors in the parameters were estimated. The uncertainty of the current study was determined as follows:

$$\text{by WR} = \sqrt{\left(\frac{\partial R}{\partial x_1}\cdot Wx_1\right)^2 + \left(\frac{\partial R}{\partial x_2}\cdot Wx_2\right)^2 + \cdot\frac{\partial R}{\partial x_n}\cdot Wx_n} \quad (1)$$

$$R = f(X_1, X_2, \ldots X_n) \quad (2)$$

where $X_1, X_2, \ldots X_n$ are independent variables and $Wx_1, Wx_2, \ldots Wx_n$ are the absolute uncertainties of $X_1, X_2, \ldots X_n$.

4. Heat Transfer and Pressure Drop Calculations

The experiments were conducted both in laminar and turbulent flow conditions. The overall heat transfer coefficient, friction factor and Nusselt number were determined based on the observed data during experimentation using the following expressions.

The heat absorbed by the working fluid was estimated using the following equation [29]:

$$Qa = \dot{m}Cp(\Delta T) \quad (3)$$

The collector efficiency was calculated as follows [29]:

$$\eta_c = \left[\frac{(T_2 - T_1)\cdot m_w\cdot C_p}{I\cdot A_a}\right] \quad (4)$$

The overall heat transfer coefficient under steady state flow was calculated using the following equation:

$$\frac{1}{UoAo} = \frac{1}{hiAi} + \ln\frac{\left(\frac{do}{di}\right)}{2\Pi KL} \quad (5)$$

The Nusselt number was calculated as follows:

$$\mathrm{Nu} = \frac{\mathrm{hidi}}{\mathrm{k}} \tag{6}$$

The pressure drop in the corrugated tube was found using manometer readings, and the friction factor value is calculated using the following formula:

$$\mathrm{F} = \frac{\Delta \mathrm{p}}{\frac{1}{2}\rho \mathrm{v}^2} \left(\frac{\mathrm{di}}{\mathrm{L}}\right) \tag{7}$$

5. Results and Discussion

Experimental works were performed on the newly modified experimental setup. Initially, the experiments were carried out in a plain tube absorber at different flow conditions. The friction factor values were estimated and compared with the Darcy-Weisbach Equation (8).

$$\Delta \mathrm{P}/l = f\frac{\mathrm{V}^2\rho}{2Di} \tag{8}$$

Both the experimental and theoretical values almost matched at regular intervals, as shown in Figure 5.

$$\mathrm{N} = \frac{\mathrm{hiDi}}{\mathrm{k}} \tag{9}$$

$$\mathrm{Nu} = 0.023\ \mathrm{Re}^{0.08}\ \mathrm{Pr}^{\mathrm{n}} \tag{10}$$

The estimated values based on the experimental observations coincided almost perfectly with the theoretical findings. This indicated that the constructed experimental setup and its working performance were good.

The estimated values of the Nusselt number for the different mass flow rates were compared with the Dittus-Boelter Equation (10); the results matched well, as shown in Figure 6. The increased Reynolds number enhanced the degree of turbulence and led to an increased heat transfer rate, as shown in Figure 7. The corrugated tube changed the direction of fluid flow which, in turn, increased the convective heat transfer. Increased Nu values were achieved by decreasing the pitch of the conical strip insert (I_3). The inserts changed the direction of flow. The corrugated tube with I_3 had the maximum value of the Nusselt number due to the additional swirl effect resulting from the geometry of the corrugations [30–32]. The increased Reynolds number enhanced the degree of turbulence and led to an increased heat transfer rate, as shown in Figure 8. The corrugated tube produced the turbulence effect in the water, which in turn increased the convective heat transfer rate. The increased Nu values were achieved further due to the additional turbulence effect caused by decreasing the pitch of the conical strip inserts. The plain tube absorber temperature was high compared to a combination of different pitches of inserts in the corrugated tube, as shown in Figure 9. It showed that water absorbed less heat from the wall in the case of the plain tube. The corrugated tube fitted with I_3 has a lower value of absorber temperature due to the increased transfer of heat to the working fluid caused by extra turbulence. Figure 10 showed that the friction factor values decreased gradually with an increase in the Re number for all the configurations. A U-tube manometer measured the pressure of water at the entry and exit of the receiver. The friction factor values are calculated. The pressure drop was high for the combination of the corrugated tube with a 20-mm pitch of conical strip insert (I_3) due to the maximum swirl effect achieved by the use of a low-pitch insert. The plain tube has less instantaneous efficiency due to the minimum utilization of solar energy, whereas the corrugated tubes have increased efficiency. It is caused by the turbulence created by the geometry. The use of inserts in the corrugated tube increased efficiency even further. The optimized corrugated tube CT_3 with I_3 provides the maximum instantaneous efficiency due to the maximum absorption of heat energy by water due to increased turbulence in the working fluid, which in turn increases the heat

transfer as shown in Figure 11. The thermal efficiency of CT-I_3 increased by 8% compared with the plain tube, as shown in Figure 12.

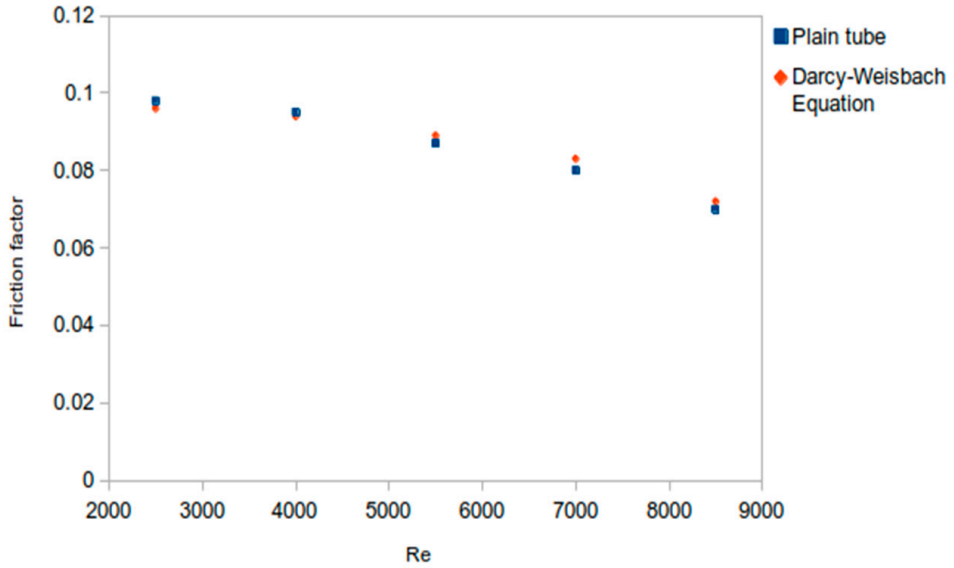

Figure 5. Variation of friction factor with the Reynolds number.

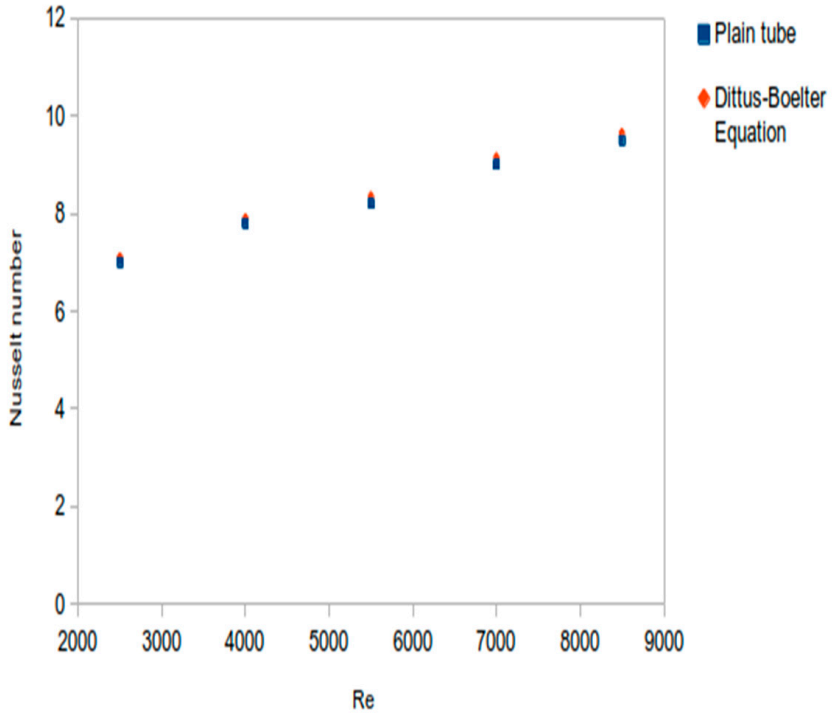

Figure 6. Variation of Nusselt number with the Reynolds number.

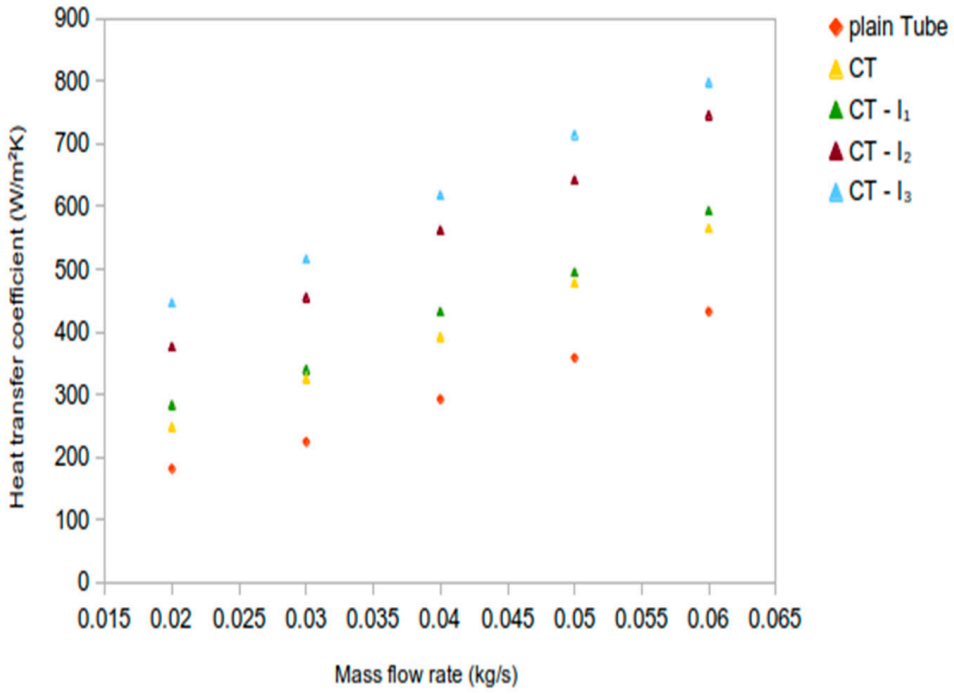

Figure 7. Variation of heat transfer coefficient with mass flow rate.

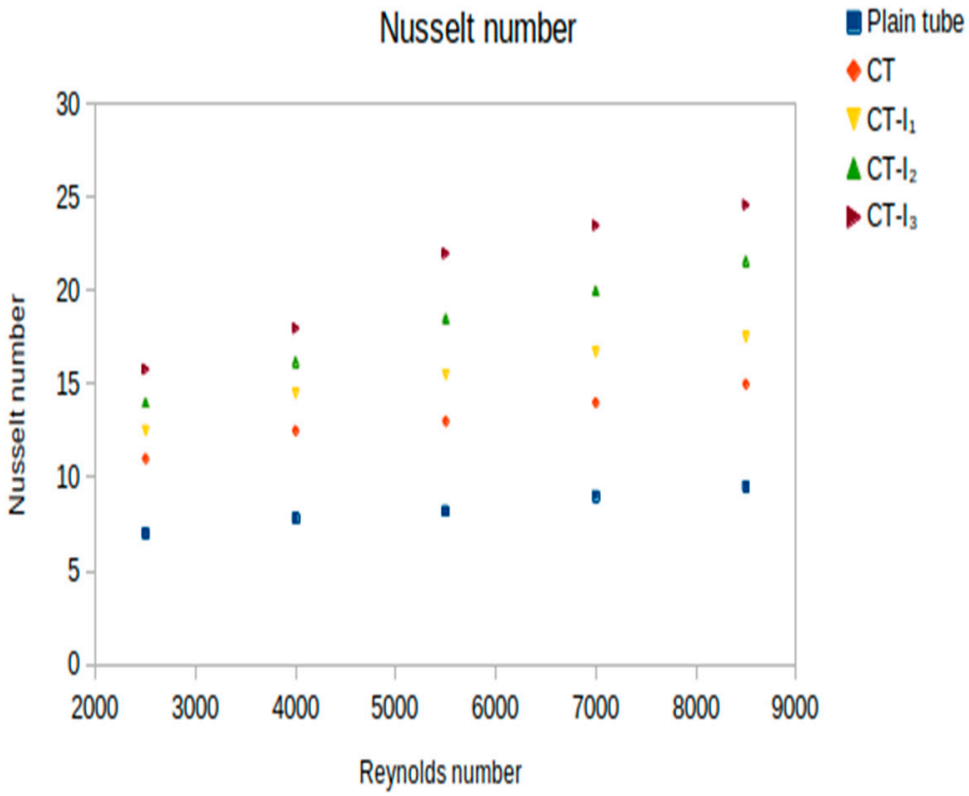

Figure 8. Variation of Nusselt number with flow rates for various absorbers. (CT-I_1 (p_i = 50 mm), CT-I_2 (p_i = 30 mm), CT-I_3 (p_i = 20 mm)).

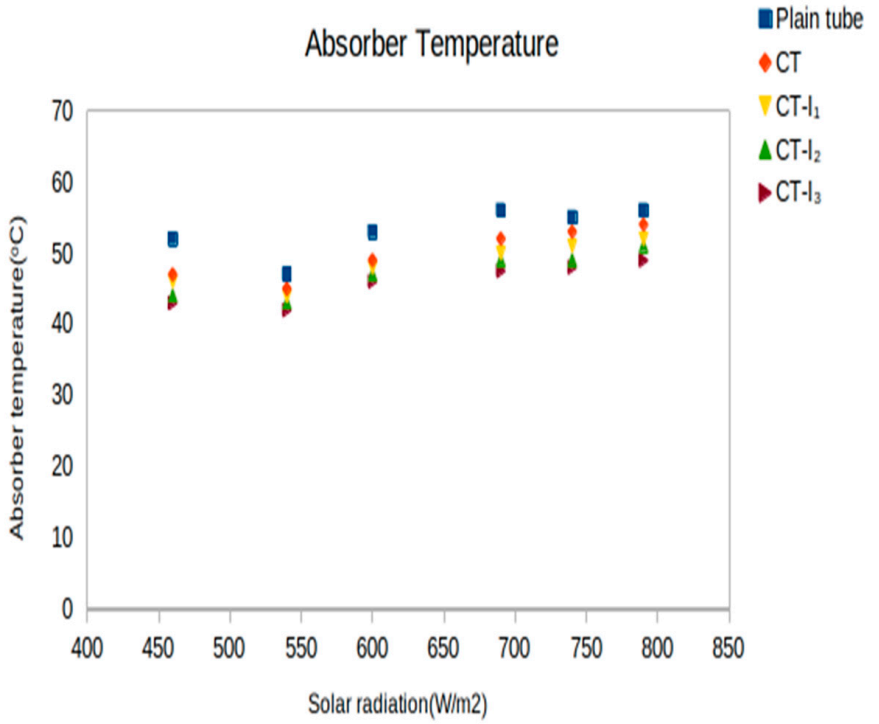

Figure 9. Variation of absorber temperatures during the day for various absorbers.

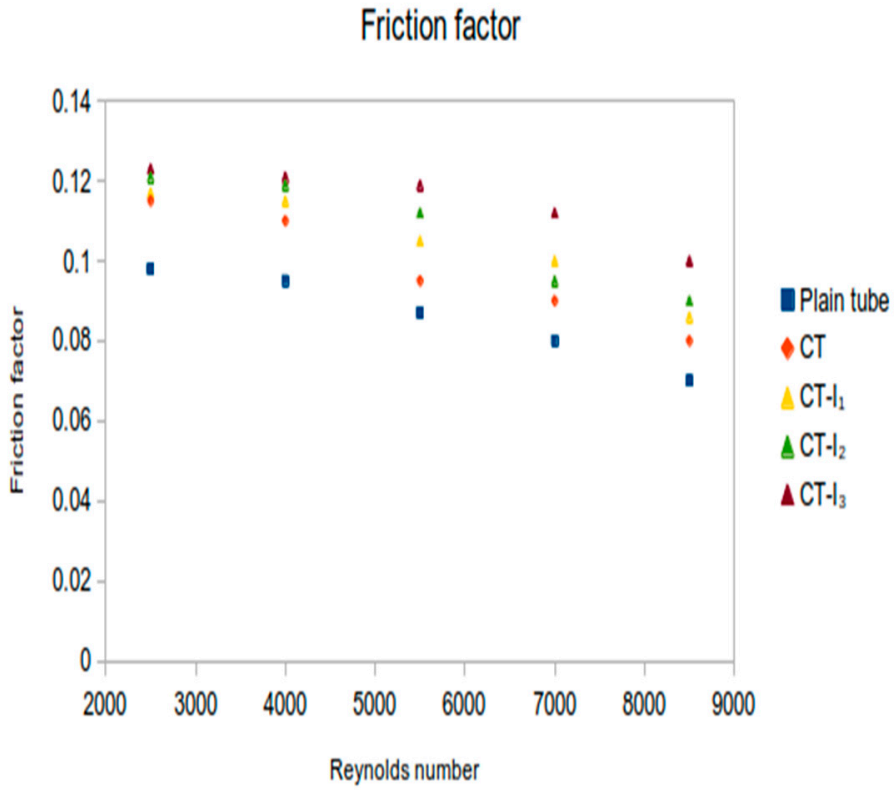

Figure 10. Variation of friction factor with flow rates for various absorbers.

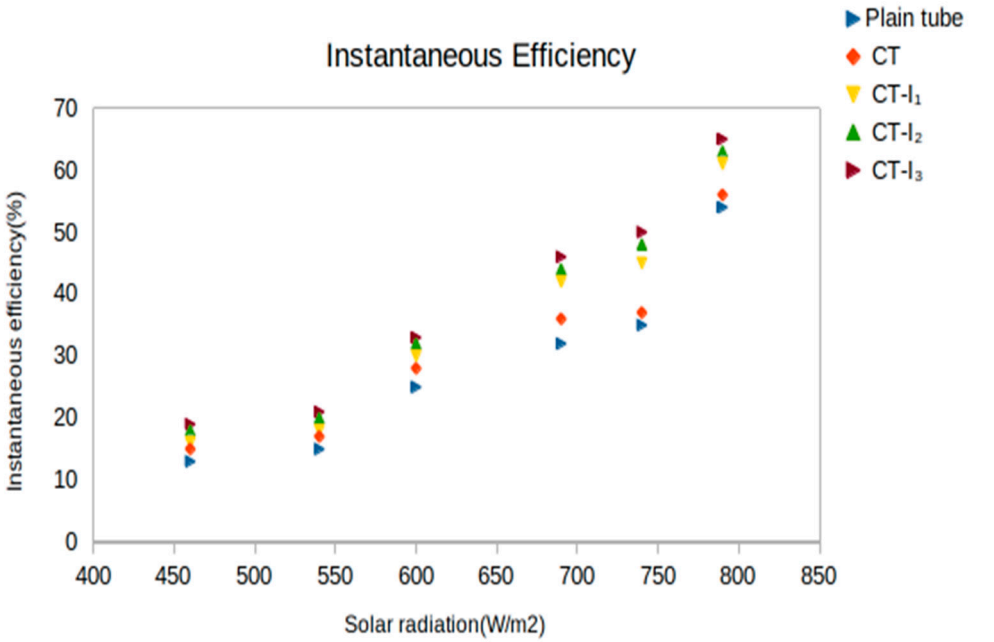

Figure 11. Variation of instantaneous efficiency during the day for various absorbers.

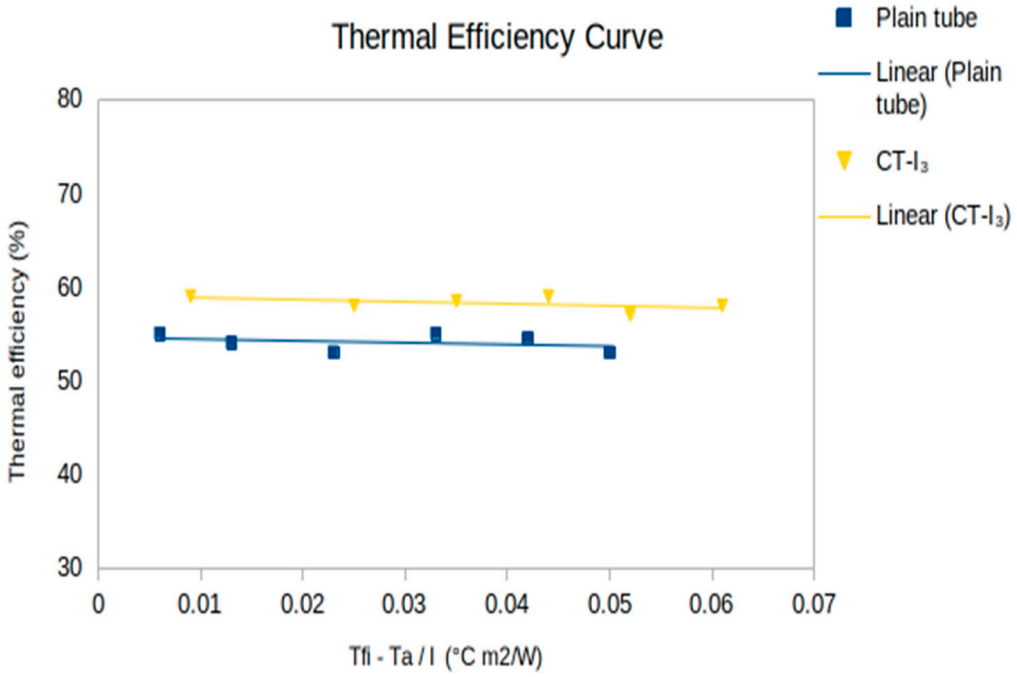

Figure 12. Comparison of thermal efficiency of plain tube with CT-I_3.

6. Linear Regression Model (Scikit-Learn)

The experimental observations, as shown in Table 4, were used to establish the analytical linear regression model using the Scikit-Learn library in the Python programming language. Additionally, the output parameters such as friction factor and Nu number were correlated with the continuous input of the Re number. A correlogram is presented in Figure 13.

Table 4. Data used for LR model.

Statistical Attributes	Reynolds Number	Nusselt Number	Friction Factor
count	15	15	15
mean	5500	18.26	0.1158
std	2195.78	3.52	0.0075
min	2500	13	0.1
25%	4000	15.9	0.1115
50%	5500	18	0.115
75%	7000	21	0.122
max	8500	24.6	0.126

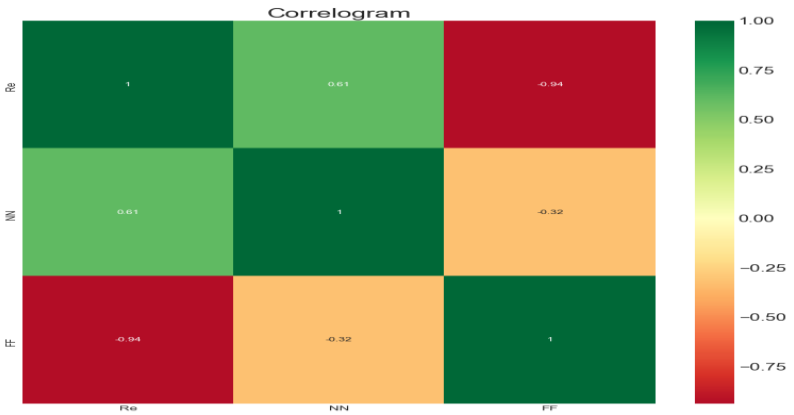

Figure 13. Correlogram of the input and outputs.

A total of 15 entries of inputs, such as the Re number and various pitches of inserts, were used for the prediction of the Nu number and friction factor, respectively. Among the 15 data points, 12 were used for training and 3 were used for testing the developed models. The LR algorithm is a very popular machine-learning modelling technique and the performance evaluation of the model is shown in Table 5. The mathematical equation of LR is as follows:

$$Y = C + mX \quad (11)$$

Table 5. Performance evaluation of the model.

ML Model	Friction Factor				Nusselt Number			
	R^2	MSE	RMSE	MAE	R^2	MSE	RMSE	MAE
LR algorithm	0.95	0.00002	0.00458	0.00374	0.94	0.99309	0.99658	0.87264

The experimental values were compared with the predicted output values and presented in graphical form, as shown in Figures 14 and 15.

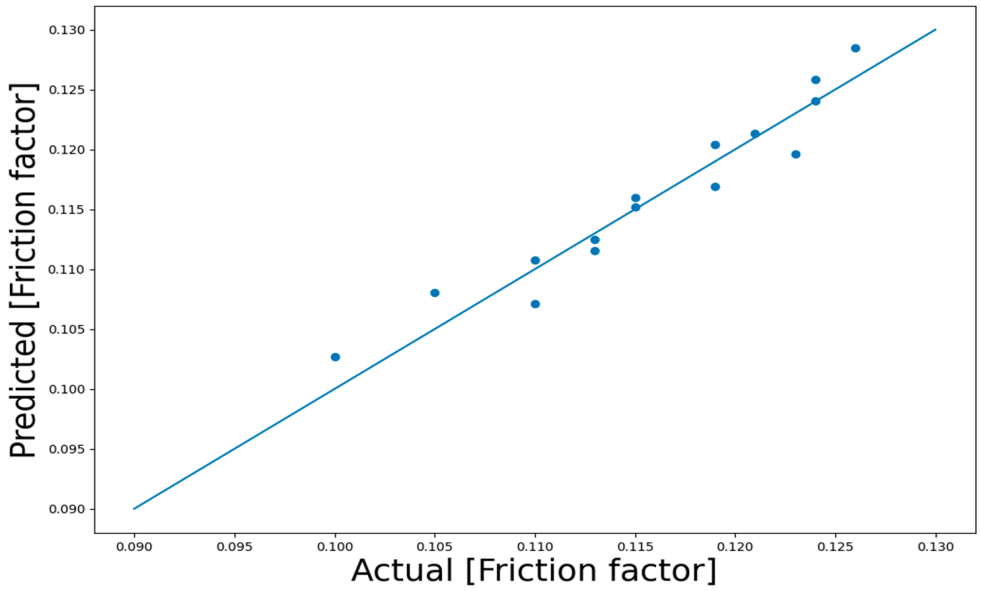

Figure 14. Actual and LR-predicted friction factor.

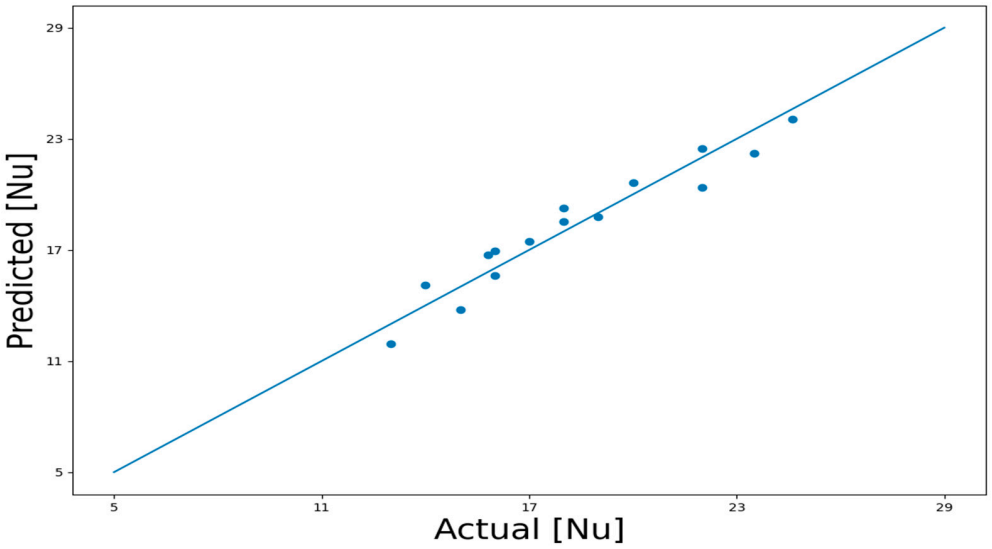

Figure 15. Actual and LR predicted Nu number.

The experimental friction factor values were plotted against the LR-predicted values. It can be concluded that the model did a good job of predicting the FF, i.e., with almost 95% accuracy. The Nusselt numbers were also predicted using the LR-developed models. The actual and predicted values of the Nu number were plotted and are presented in Figure 15. As shown, the LR predicted the Nu number with an accuracy of 93%. The actual and predicted values of absorber temperature and heat transfer coefficient are presented in Figures 16 and 17. The LR predicted the absorber temperature and heat transfer coefficient with an accuracy of 94% and 98.5%, respectively.

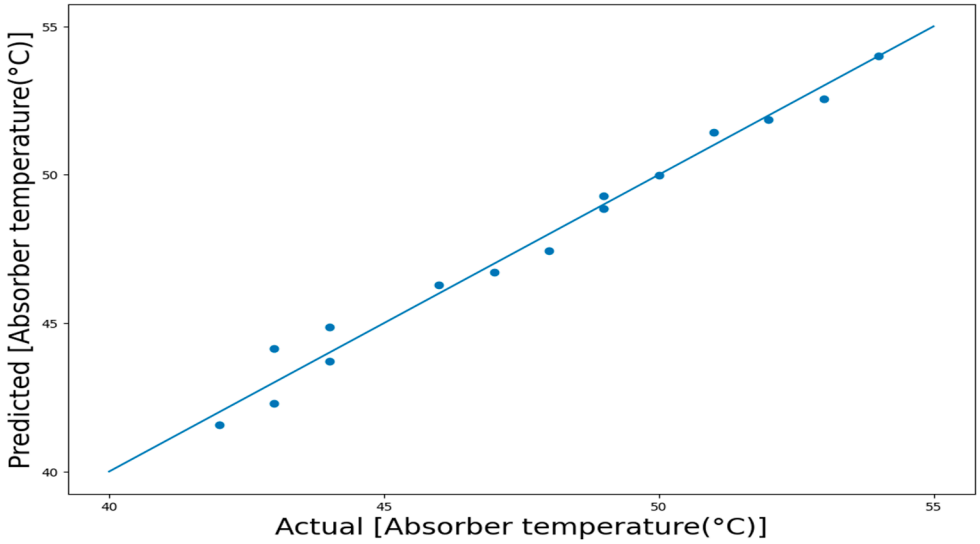

Figure 16. Actual and LR predicted Absorber temperature.

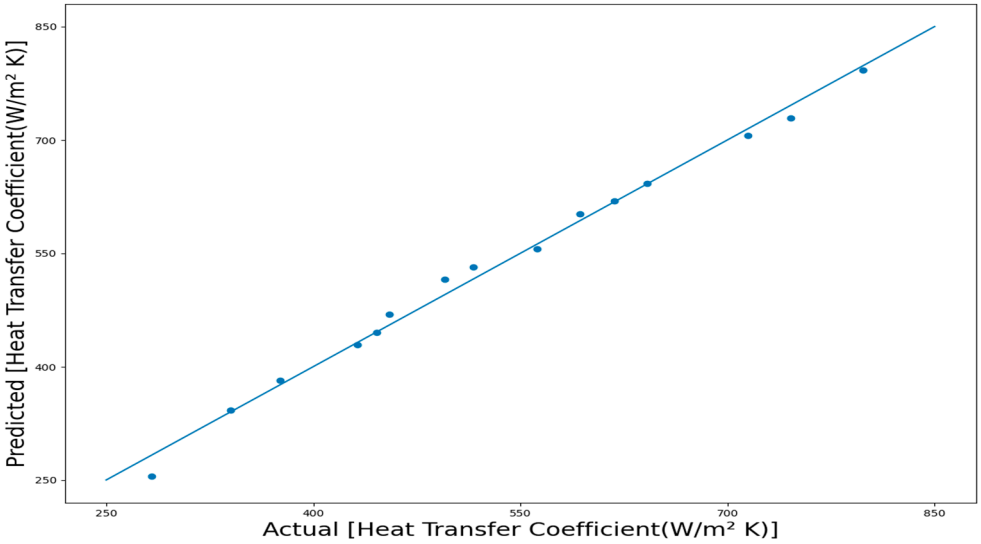

Figure 17. Actual and LR predicted Heat transfer coefficient.

7. Conclusions

1. Experiments were carried out on a solar PTC using a corrugated tube absorber with conical strip inserts; the following conclusions may be made.
2. The highest thermal performance, friction factor value, convective heat transfer and Nusselt number value were achieved using a combination of CT with I3. The highest friction factor value was achieved using CT-I3; it was 38% higher compared to that obtained using a plain tube and 25% higher compared to that with CT without insert. The Nusselt value increased to a maximum of 177% compared to that of the plain tube and 78% compared to the CT.
3. The maximum convective heat transfer coefficient value of CT-I3 was 798W/m^2K, i.e.,84.72% higher than that obtained with the plain tube and 41.23% higher compared to the CT without an insert.
4. The instantaneous efficiency of CT with I3was 26.92% higher than that obtained with the plain tube and 13.79% compared to the CT under the same working conditions.
5. A maximum thermal efficiency of 59% was achieved using CT with I3, while 55% was achieved while using the plain tube.

6. The best results were achieved using the combination of corrugated tube CT (hc = 2 mm, pi = 8 mm) and conical strip insert I3 (20 mm).
7. The LR model was developed with the help of the experimental values obtained via the Scikit-Learn library in the Python programming language. The friction factor and the Nusselt number were predicted with an accuracy of 95% and 93%, respectively. Therefore, the analytical model matched the performance of the experimental model extremely well.
8. The friction factor, Nusselt number, absorber temperature and heat transfer coefficient were predicted with accuracies of 95%, 93%, 94% and 98.5%, respectively. Therefore, again, the analytical model matched the performance of the experimental model extremely well.

Author Contributions: Conceptualization, R.V.; Formal analysis, K.S.J.; Funding acquisition, M.A. and C.A.S.; Investigation, E.C. and S.S.; Methodology, P.V.E., E.C. and M.A.; Resources, S.S. and C.A.S.; Software, E.C.; Supervision, E.C.; Visualization, S.S.; Writing—original draft, R.V., E.C. and S.S.; Writing—review & editing, K.S.J., S.S. and M.A. All authors have read and agreed to the published version of the manuscript.

Funding: This research was funded by the Deanship of Scientific Research at King Khalid University (Grant No: RGP 1/349/43).

Institutional Review Board Statement: Not applicable.

Informed Consent Statement: Not applicable.

Data Availability Statement: Not applicable.

Acknowledgments: The authors extend their appreciation to the Deanship of Scientific Research at King Khalid University, Saudi Arabia for funding this work through Research Group Program under Grant No: RGP. 1/349/43.

Conflicts of Interest: The authors declare no conflict of interest.

Nomenclature

Ao	Outer surface area (m^2)
Ai	Inner surface area (m^2)
C_p	Specific heat of water (J/kgK)
d_i	Absorber tube inner diameter (m)
d_o	Absorber tube outer diameter (m)
f	Friction factor
h	Convective heat transfer coefficient (W/m^2 K)
K	Thermal conductivity (W/m K)
l	Length of the absorber tube (m)
m	Mass flow rate of fluid (kg/s)
Nu	Nusselt number
ρ	Density of fluid (kg/m^3)
Δp	Pressure drop (N/m^2)
Q	Heat transfer rate (W)
Re	Reynolds number
Ti	Fluid inlet temperature (°K)
To	Fluid outlet temperature (°K)
U	Overall heat transfer coefficient (W/m^2K)
V	Velocity (m/s)
Y	Twist ratio

References

1. Hashim, W.M.; Shomran, A.T.; Jurmut, H.A.; Gaaz, T.S.; Kadhum, A.A.H.; Al-Amiery, A.A. Case study on solar water heating for flat plate collector. *Case Stud. Therm. Eng.* **2018**, *12*, 666–671. [CrossRef]
2. Pandey, K.M.; Chaurasiya, R. A review on analysis and development of solar flat plate collector. *Renew. Sustain. Energy Rev.* **2017**, *67*, 641–650. [CrossRef]
3. Cunio, L.; Sproul, A. Performance characterisation and energy savings of uncovered swimming pool solar collectors under reduced flow rate conditions. *Sol. Energy* **2012**, *86*, 1511–1517. [CrossRef]
4. Bunea, M.; Perers, B.; Eicher, S.; Hildbrand, C.; Bony, J.; Citherlet, S. Mathematical modelling of unglazed solar collectors under extreme operating conditions. *Sol. Energy* **2015**, *118*, 547–561. [CrossRef]
5. Soltau, H. Testing the thermal performance of uncovered solar collectors. *Sol. Energy* **1992**, *49*, 263–272. [CrossRef]
6. Katsaprakakis, D.A. Computational Simulation and Dimensioning of Solar-Combi Systems for Large-Size Sports Facilities: A Case Study for the Pancretan Stadium, Crete, Greece. *Energies* **2020**, *13*, 2285. [CrossRef]
7. Katsaprakakis, D.A.; Zidianakis, G. Optimized Dimensioning and Operation Automation for a Solar-Combi System for Indoor Space Heating. A Case Study for a School Building in Crete. *Energies* **2019**, *12*, 177. [CrossRef]
8. Arnaoutakis, G.E.; Katsaprakakis, D.A. Concentrating Solar Power Advances in Geometric Optics, Materials and System Integration. *Energies* **2021**, *14*, 6229. [CrossRef]
9. Rawani, A.; Sharma, S.P.; Singh, D.P. Comparative performance analysis of different twisted tape inserts in the absorber tube of parabolic trough collector. *Trans. Stellar* **2018**, *8*, 643–656.
10. Arun George, E.R.; Vinayprakash, E.; Rai, A.K. Fabrication and performance of solar parabolic trough concentrator with and without coating on receiver tube. *Transstellar* **2017**, *7*, 431–438. [CrossRef]
11. Alexander, J.M.; Kueffer, C.; Daehler, C.; Edwards, P.J.; Pauchard, A.; Seipel, T.; Arévalo, R.J.; Cavieres, L.A.; Dietz, H.; Jakobs, G.; et al. Assembly of nonnative floras along elevational gradients explained by directional ecological filtering. *Proc. Natl. Acad. Sci. USA* **2011**, *108*, 656–661. [CrossRef]
12. Diwan, K.; Soni, M.S. Heat Transfer Enhancement in Absorber Tube of Parabolic Trough Concentrators Using Wire-Coils Inserts. *Univers. J. Mech. Eng.* **2015**, *3*, 107–112. [CrossRef]
13. Çağlar, A. Design of a Parabolic Trough Solar Collector Using a Concentrator with High Reflectivity. In Proceedings of the 2nd World Congress on Mechanical, Chemical, and Material Engineering (MCM'16), Budapest, Hungary, 22–23 August 2016. [CrossRef]
14. Kalidasan, B.; Shankar, R.; Srinivas, T. Absorber Tube with Internal Hinged Blades for Solar Parabolic Trough Collector. *Energy Procedia* **2016**, *90*, 463–469. [CrossRef]
15. Yousif, A.H.; Khudhair, M.R. Enhancement of Heat Transfer in a Tube Fitted with Passive Technique as Twisted Tape Insert—A Comprehensive Review. *Am. J. Mech. Eng.* **2019**, *7*, 20–34.
16. Jamal-Abad, M.T.; Saedodin, S.; Aminy, M. Experimental investigation on a solar parabolic trough collector for absorber tube filled with porous media. *Renew. Energy* **2017**, *107*, 156–163. [CrossRef]
17. Younas, T.; Bano, N.; Khalid, M.A. *An Experimental Study of Modelling and Fabrication of an Autonomous Solar Parabolic Trough Collector*; IEEE: Piscataway, NJ, USA, 2018; ISBN 978-1-5386-7939-5/978-1-5386-7938-8/978-1-5386-7940-1.
18. Aravind, G.; Yadav, R.K.; Loganathan, C.; Sharma, S. Experimental investigation of cavity absorber in parabolic solar collector. In Proceedings of the 2016 International Conference on Recent Advances and Innovations in Engineering (ICRAIE), Jaipur, India, 23–25 December 2016; pp. 1–5. [CrossRef]
19. Aldulaimi, R.K.M. An Innovative Receiver Design for a Parabolic Trough Solar Collector Using Overlapped and Reverse Flow: An Experimental Study. *Arab. J. Sci. Eng.* **2019**, *44*, 7529–7539. [CrossRef]
20. Norouzi, A.M.; Siavashi, M.; Oskouei, M.K. Efficiency enhancement of the parabolic trough solar collector using the rotating absorber tube and nanoparticles. *Renew. Energy* **2019**, *145*, 569–584. [CrossRef]
21. Anbu, S.; Venkatajalapathy, S.; Suresh, S. Convective heat transfer studies on helically corrugated tubes with spiraled rod inserts using TiO2 / DI water nanofluids. *J. Therm. Anal. Calorim.* **2019**, *137*, 849–864. [CrossRef]
22. Almeshaal, M.; Arunprasad, V.; Palaniappan, M.; Kolsi, L. Experimental study of a solar water heater fitted with spacer at the leading edge of Left-Right screw tapes. *Case Stud. Therm. Eng.* **2020**, *22*, 100777. [CrossRef]
23. Mwesigye, Y.A.; Goksu, T.T. Enhancing the ovarall thermal performance of a large aperture SPTC using wire coil inserts. *Sustain. Energy Technol. Assess.* **2020**, *39*, 100696.
24. Kumar, B.N.; Reddy, K. Numerical investigations on metal foam inserted solar parabolic trough DSJ absorber tube for mitigating thermal gradients and enhancing heat transfer. *Appl. Therm. Eng.* **2020**, *178*, 115511. [CrossRef]
25. Wongcharee, K.; Eiamsaard, S. Heat transfer enhancement by using CuO/water nanofluid in corrugated tube equipped with twisted tape. *Int. Commun. Heat Mass Transf.* **2012**, *39*, 251–257. [CrossRef]
26. Valenzuela, L.; Setien, E.; Zarza, E. Analysis of a failure mechanism in parabolic troughs receivers due to bellows cap overirradiation. *Eng. Fail. Anal.* **2020**, *111*, 104491. [CrossRef]
27. Arnaoutakis, G.E.; Katsaprakakis, D.A.; Christakis, D.G. Dynamic modeling of combined concentrating solar tower and parabolic trough for increased day-to-day performance. *Appl. Energy* **2022**, *323*, 119450. [CrossRef]
28. Holman, J.P. *Experimental Methods for Engineers*, 7th ed.; McGraw-Hill: New York, NY, USA, 2001.
29. Kalogirou, S. *Solar Energy Engineering: Process and Systems*, 1st ed.; Elsevier: London, UK, 2009.

30. Saravanan, A.; Murugan, M.; Reddy, M.S.; Kumar, P.; Elumalai, P.V. Performance Enhancement of Tubular Solar Still With Various Rotating Wicked Materials—An Experimental Approach. *J. Therm. Sci. Eng. Appl.* **2022**, *14*, 1–22. [CrossRef]
31. Murugan, M. An overview on energy and exergy analysis of solar thermal collectors with passive performance enhancers. *Alex. Eng. J.* **2022**, *61*, 8123–8147. [CrossRef]
32. Saravanan, A.; Murugan, M.; Reddy, M.S.; Ranjit, P.; Elumalai, P.; Kumar, P.; Sree, S.R. Thermo-hydraulic performance of a solar air heater with staggered C-shape finned absorber plate. *Int. J. Therm. Sci.* **2021**, *168*, 107068. [CrossRef]